

1 **Hot-melt extruded filaments based on pharmaceutical grade polymers for 3D**
2 **printing by Fused Deposition Modeling**

3 Alice Melocchi^a, Federico Parietti^b, Alessandra Maroni^a, Anastasia Foppoli^a, Andrea Gazzaniga^a,
4 Lucia Zema^{a*}

5
6 ^aUniversità degli Studi di Milano, Dipartimento di Scienze Farmaceutiche, Sezione di Tecnologia e
7 Legislazione Farmaceutiche "M.E. Sangalli", Via G. Colombo 71, 20133 Milan, Italy;
8 alice.melocchi@unimi.it, alessandra.maroni@unimi.it, anastasia.foppoli@unimi.it,
9 andrea.gazzaniga@unimi.it

10 ^bMassachusetts Institute of Technology, Mechanical Engineering Department, 77 Massachusetts
11 Ave, Cambridge US-MA 02139; parietti@mit.edu

12
13
14 *Corresponding author: L. Zema; Telephone: +39-02-503-24654;

15 E-mail: lucia.zema@unimi.it
16

17 **Abstract**

18 Fused deposition modeling (FDM) is a 3D printing technique based on the deposition of successive
19 layers of thermoplastic materials following their softening/melting. Such a technique holds huge
20 potential for the manufacturing of pharmaceutical products and is currently under extensive
21 investigation. Challenges in this field are mainly related to the paucity of adequate filaments
22 composed of pharmaceutical grade materials, which are needed for feeding the FDM equipment.
23 Accordingly, a number of polymers of common use in pharmaceutical formulation were evaluated
24 as starting materials for fabrication via hot melt extrusion of filaments suitable for FDM processes.
25 By using a twin-screw extruder, filaments based on insoluble (ethylcellulose, Eudragit[®] RL),
26 promptly soluble (polyethylene oxide, Kollicoat[®] IR), enteric soluble (Eudragit[®] L, hydroxypropyl
27 methylcellulose acetate succinate) and swellable/erodible (hydrophilic cellulose derivatives,
28 polyvinyl alcohol, Soluplus[®]) polymers were successfully produced, and the possibility of
29 employing them for printing 600 µm thick disks was demonstrated. The behavior of disks as
30 barriers when in contact with aqueous fluids was shown consistent with the functional application
31 of the relevant polymeric components. The produced filaments were thus considered potentially
32 suitable for printing capsules and coating layers for immediate or modified release, and, when
33 loaded with active ingredients, any type of dosage forms.

34

35

36

37

38

39 **Keywords:** 3D printing, fused deposition modeling, hot melt extrusion, filament, pharmaceutical
40 grade polymer, drug delivery system

41

42 **1. Introduction**

43 Some major challenges that still have to be faced in the field of drug delivery (*e.g.* drug targeting,
44 administration of proteins, personalized therapy) and pharmaceutical production (*e.g.* continuous
45 manufacturing, optimization) relate to the development and proper application of new
46 manufacturing techniques, such as hot-processing including hot melt extrusion (HME), injection
47 molding (IM) and 3D printing (3DP) by fused deposition modeling (FDM) (Maroni et al., 2012;
48 Park, 2015; Mascia et al., 2013, Melocchi et al, 2015a; Norman et al., 2016; Shah et al., 2013; Zema
49 et al., 2012). As far as 3DP is concerned, it has gained huge interest in recent years after finding
50 widespread application in many industrial domains (*e.g.* automotive, aerospace, fashion and
51 defense), where it is also exploited as a rapid prototyping tool. In this respect, it allows a
52 representation of an item to be created before its final release or commercialization, thus reducing
53 time and costs of the development. Moreover, 3DP turned out to be promising in the biomedical
54 field for producing personalized prostheses on the basis of each patient's characteristics and needs,
55 as identified by imaging techniques (*e.g.* x-ray computed tomography, nuclear magnetic resonance)
56 (Rengier et al., 2010). 3DP includes a variety of techniques (*e.g.* stereolithography, selective laser
57 sintering, fused deposition modeling). They all enable the fabrication of objects starting from digital
58 models through the addition of successive layers (*i.e.* additive manufacturing), while differing in the
59 starting materials and additive processes employed (Gibson et al. 2010; Pham and Gault, 1998).

60 3DP based on both powder solidification, first developed at Massachusetts Institute of Technology,
61 and extrusion, was recently proposed for the development of drug products (Norman et al., 2016;
62 Prasad and Smyth, 2015; Yu et al., 2008). Indeed, in 2015 the first 3D printed drug product
63 (Spritam[®]) was approved by US Food and Drug Administration agency (FDA)
64 ([http://www.drugs.com/newdrugs/fda-approves-spritam-levetiracetam-first-3d-printed-product-](http://www.drugs.com/newdrugs/fda-approves-spritam-levetiracetam-first-3d-printed-product-4240.html)
65 [4240.html](http://www.spritam.com); <http://www.spritam.com>). It is a tablet that can be loaded with differing doses (up to
66 1000 mg) of levetiracetam, manufactured through the Aprexia's ZipDose[®] technology. This exploits

67 3DP by powder solidification to produce a porous orodispersible formulation that rapidly
68 disintegrates in a very low amount of liquid.

69 FDM is an extrusion-based 3DP technique easily accessible, low-cost, versatile and characterized
70 by a good potential for fabrication of single-unit dosage forms (Goyanes et al., 2015a; Norman et
71 al., 2016; Yu et al., 2008). It allows the type, dose, and distribution of the active ingredient as well
72 as the size, shape, geometry (*e.g.* hollow, multi-layer, coated) and density of the final product to be
73 varied, thus ideally meeting the needs of personalized medicine (Goyanes et al., 2015b and c;
74 Melocchi et al., 2015b; Skowrya et al., 2015). FDM consists in the deposition, on a build plate, of
75 molten/softened materials from a heated printer extrusion head that moves along the x and y axes,
76 while lowering of the build plate enables the growth of the item bottom-up (Gibson et al., 2010).

77 Starting materials are generally supplied in the form of filaments, which are produced by HME. The
78 first commercially available filaments were mainly based on acrylonitrile butadiene styrene (ABS)
79 and polylactic acid (PLA). Because of the increasing interest in FDM, the fabrication of filaments
80 has become an important research area. Therefore, not only the use of other materials was explored,
81 *e.g.* polyvinyl alcohol (PVA), XT copolyester, polyethylene terephthalate, nylon, thermoplastic
82 polyurethane, but also different physical/mechanical properties of filaments (*e.g.* color, resistance,
83 flexibility) were pursued. In the pharmaceutical field, early attempts were carried out using plastics
84 (*e.g.* ethylene vinyl acetate, PLA, PVA) also in the form of filaments available on the market,
85 introducing the active ingredient by soaking or extrusion (Genina et al., 2016; Goyanes et al., 2014;
86 Goyanes et al., 2015a, b, c and d; Holländer, et al., 2016; Sandler et al., 2014; Skowrya et al., 2015;
87 Water et al., 2015). Only very recently, a few drug-containing monolithic units intended for oral
88 administration were described based on purposely-extruded filaments (Pietrzak et al., 2015).

89 Moreover, starting from filaments based on hydroxypropyl cellulose (HPC), hollow items in the
90 form of caps and bodies to be assembled in a capsule shell for pulsatile release were prepared
91 (Melocchi et al., 2015b). FDM was also demonstrated a suitable prototyping tool for
92 swellable/erodible capsular delivery platforms prepared by IM (Gazzaniga et al., 2011; Macchi et

93 al., 2015; Melocchi et al., 2015b; Zema et al., 2013a). However, few thermoplastic materials were
94 investigated so far, none of which is commercially available as filaments. Hence, in view of the
95 variety of polymeric materials used in the manufacturing of dosage forms and DDSs, investigations
96 in this respect need to be broadened. The availability of libraries of polymeric filaments, which may
97 differ in terms of physico-technological characteristics and processing conditions while allowing
98 products with comparable performance to be obtained, could be of great interest, for instance to
99 circumvent stability issues related to the operating temperatures involved by each material.

100 Based on these premises, the aim of the present work was to produce filaments suitable for FDM
101 starting from a variety of pharmaceutical grade polymers having differing physico-chemical
102 characteristics. Particularly, insoluble, promptly soluble, enteric soluble and swellable/erodible
103 polymers were considered. Such filaments would be intended for fabrication of capsule shells and
104 coatings for either immediate or modified release. In addition, they could be loaded with active
105 ingredients and then employed for the manufacturing of printed monolithic drug products (*e.g.*
106 pellets, tablets, matrices).

107

108 **2. Materials and Methods**

109 **2.1 Materials**

110 Polylactic acid, PLA filament (L-PLA natural, \varnothing 1.75 mm; MakerBot[®] Industries, LLC, US-NY);
111 ethyl cellulose, EC (Ethocel[™] Std. 100 premium, Dow, US-MY); hydroxypropyl cellulose, HPC
112 (Klucel[®] LF, Ashland, US-NJ); hydroxypropyl methyl cellulose, HPMC (Affinisol[™] 15cP, Dow, US-
113 CA); hydroxypropyl methyl cellulose acetate succinate, HPMCAS (AQUOT-LG[®]; Shin-Etsu, J);
114 methacrylic acid copolymer Eudragit[®] L 100-55, EDR L, and Eudragit[®] RL PO, EDR RL (Evonik, D);
115 polyethylene oxide, PEO (Sentry Polyox[™] WSR N10 LEO NF, Colorcon, UK); polyvinyl alcohol,
116 PVA (Gohsenol[®] EG 05P, Nippon Goshei, J); polyvinyl alcohol-polyethylene glycol graft copolymer,
117 KIR (Kollicoat[®] IR, BASF, D); polyvinyl caprolactam-polyvinyl acetate-polyethylene glycol graft co-
118 polymer, SLP (Soluplus[®], BASF, D); glycerol, GLY (Pharmagel, I); polyethylene glycols, PEG 400 and

119 PEG 8000 (Clariant Masterbatches, I); triethyl citrate, TEC (Sigma Aldrich, D); acetaminophen, AAP
120 (Rhodia, I); furosemide, FUR (Metapharmaceutical, E).

121

122 **2.2 Methods**

123 PLA filament was used as received. All materials, except for PEGs, GLY, TEC, AAP and FUR, were
124 kept in an oven at 40 °C for 24 h prior to use. Plasticized polymeric formulations were prepared by
125 mixing polymers with the selected plasticizer in a mortar. The amount of plasticizer was expressed as %
126 by weight on the dry polymer. FUR was added to the KIR-based formulation by mixing in a mortar and
127 its amount was expressed as % by weight on the final mixture (*i.e.* 30%).

128

129 *2.1.1 Preparation of filaments*

130 Filaments were prepared by HME using a twin-screw extruder (Haake™ MiniLab II, Thermo Scientific,
131 US-WI) equipped with counter-rotating screws and a custom-made aluminum rod-shaped die ($\phi = 1.80$
132 mm); process conditions are reported in the Results section. Extruded rods were manually pulled and
133 forced to pass through a caliber connected with the extruder and set at 1.80 mm. After production,
134 filament diameter was verified every 5 cm in length and portions that had not diameter in the acceptable
135 range of 1.75 ± 0.05 mm were discarded.

136

137 *2.1.2 Printing of disks*

138 FDM was performed by an adapted MakerBot Replicator 2 equipped with a 0.4 mm tip (MakerBot®
139 Industries, US-NY; infill = 100%, layer height = 0.30 mm), using a computer-aided design (CAD) file
140 purposely developed. In particular, a disk ($\phi = 30$ mm and thickness = 600 μm) was designed using
141 Autodesk® Autocad® 2016 software version 14.0 (Autodesk, Inc., US-CA), saved in STL format and
142 imported to the 3D printer software (MakerWare Version 2.2.2.89, MakerBot® Industries, US-NY).
143 Either the supplied PLA filament or portions of at least 25 cm of the in-house prepared filaments were
144 employed.

145 The printing temperature was adapted to the thermal and mechanical behavior of each material. When
146 changing the filament before a new printing process, the printer was cleaned and leveling of the build
147 plate was performed following assembly of the heating chamber. Cleaning procedure: the temperature
148 of the heating chamber was set at 250 °C for 3 min; then it was dismantled and the material remaining
149 in the inner barrel was removed by means of a brass brush. In particular, the nozzle was unscrewed and
150 any residue inside was manually removed; then it was immersed for at least 3 h in a suitable solvent
151 depending on the solubility characteristics of the last printed material (*e.g.* water for KIR and PEO,
152 acetone for PLA).

153

154 *2.1.4 Characterization of disks*

155 Disks were stored between plates before being characterized in terms of weight (analytical balance
156 BP211, Sartorius, D; $n = 6$) and thickness (MiniTest FH7200 equipped with FH4 probe, \varnothing sphere =
157 1.5 mm, ElektroPhysik, D; $n = 6$), in order to avoid warpage phenomena. Digital photographs of
158 samples were acquired (Dino Lite Digital Microscope coupled with Dino Capture software, Dino-
159 Lite, VWR International, I).

160 Thickness was measured in 6 points for each of 3 concentric circumferences (Figure 1). Radius was
161 of 4mm, 7.5 mm and 13 mm for the inner, intermediate and outer circumference, respectively.
162 Values were reported as mean and the coefficient of variation (CV) was calculated.

163 Mass loss test was carried out by a six-position disintegration apparatus (900 mL of distilled water
164 for KIR, HPC, HPMC, PVA, SLP and EDR RL disks; 2 h in HCl 0.1 N and then pH 6.8 phosphate
165 buffer, according to Dissolution test for delayed-release dosage forms, Method B, USP 38, for EDR
166 L and HPMCAS disks; 37 ± 0.5 °C; 31 cycles/min). Before testing, disks were die-cut into smaller
167 ones ($\varnothing = 11$ mm) and each of them was checked for weight (initial weight, w_i) and inserted into a
168 single basket-rack assembly. At pre-determined time points, samples ($n = 3$) were withdrawn, gently
169 blotted and weighed (wet weigh, w_w). Final dry weights (w_d) were then determined after oven-

170 drying (40 °C) to constant weight. The water uptake percentage (% WU) and residual dry mass
171 percentage (% RDM) were calculated according to the following equations:

172

$$173 \quad \% WU = \left[\left(\frac{w_w - w_d}{w_w} \right) \times 100 \right] \quad \text{eq. 1}$$

174

$$175 \quad \% RDM = \left[\left(\frac{w_d}{w_i} \right) \times 100 \right] \quad \text{eq. 2}$$

176

177 Disks were also tested for barrier performance (n = 3). For this purpose, they were mounted to close
178 manually-assembled cells (area exposed to the medium = 177 mm²) (Figure 2) (Zema et al., 2013b).
179 When testing polymeric disks the donor reservoir compartment was filled with 100 mg of AAP powder
180 as a tracer (Giordano et al., 2005). The test was performed in a USP 38 dissolution apparatus 2
181 (Dissolution System 2100B, Distek, US-MA; 900 mL of medium, 100 rpm, 37 ± 0.5 °C). Fluids were
182 the same as for the mass loss test. Fluid samples were withdrawn at fixed time points and drug was
183 assayed by spectrophotometer (Lambda25, Perkin Elmer, US-MA; 254 nm). The time to 10% recovery
184 from the acceptor fluid (t_{10%}) was calculated by linear interpolation of the experimental data
185 immediately before and after this release %. In the case of enteric-soluble polymers t_{10%} was calculated
186 after the pH change.

187 t_{10%} data relevant to swellable/erodible polymer barriers were used to calculate the time equivalent
188 thickness parameter (TETP) according to the following equation (Sangalli et al., 2004):

$$TETP = \frac{\text{disk thickness}}{t_{10\%}}$$

189

190 where disk thickness is the mean of values measured along the inner and central circumferences (n =
191 12), in order to consider the surface exposed to the medium only. This parameter expresses the thickness
192 of the barrier (µm) needed to attain a unit of lag time (min).

193 Disks containing FUR and double-disk items were mounted to close the above-mentioned cells, wherein
194 the donor reservoir compartment was left empty. The test was performed in a USP 38 dissolution
195 apparatus 2 (Dissolution System 2100B, Distek, US-MA; 1000 mL of medium, 100 rpm, 37 ± 0.5 °C),
196 under sink conditions. The FUR-containing disk was tested in pH 6.8 phosphate buffer, while the fluids
197 used to test double-disk items were in those indicated in the Dissolution test for delayed-release dosage
198 forms, Method B, USP 38. Fluid samples were withdrawn at fixed time points and drug was assayed by
199 spectrophotometer (Lambda25, Perkin Elmer, US-MA; 274 nm).

200

201 **3. Results and Discussion**

202 **3.1 Extrusion of filaments and printing of disks**

203 A variety of pharmaceutical grade polymers with different functional applications and a potential
204 for hot-processing was selected for the manufacturing of filaments by HME. In particular, the use of
205 a number of promptly soluble (*i.e.* KIR, PEO), enteric soluble (*i.e.* HPMCAS, EDR L),
206 swellable/erodible (*i.e.* HPC, HPMC, PVA, SLP) and insoluble (*i.e.* EC, EDR RL) selected
207 polymers was explored.

208 The formulation and processing conditions that would allow filaments suitable for feeding a
209 commercially-available FDM equipment were investigated. A desktop, user-friendly printer,
210 MakerBot Replicator 2, designed to work with PLA filaments and equipped with a standard 0.4 mm
211 tip, was employed for 3DP processes. Disk-shaped items of 600 μm in thickness were identified as
212 viable specimens for the screening of materials. Indeed, though requiring a simple CAD file to be
213 designed, they could both highlight challenges in filament deposition on account of the limited
214 thickness/diameter ratio, and provide preliminary information on the achievable performance.
215 Notably, the possibility of producing thin items having narrow thickness tolerance ranges is of
216 utmost importance in the pharmaceutical field, especially for the manufacturing of coated dosage
217 forms or capsular devices.

218 In order to explore the feasibility of items having such features, initial trials were performed using
219 the supplied Makerbot PLA filament and standard printing conditions in compliance with the
220 technical specifications of the equipment. Based on the CAD file developed, the disks were
221 automatically fabricated through the addition of two successive layers, the latter being deposited
222 onto the former perpendicularly on the horizontal plane as envisaged by the 3D printer software.
223 Prior to each printing step, the build plate needs to be manually levelled, by setting its distance from
224 the nozzle. Because this operation appeared potentially critical to the vertical growth of the object,
225 its impact on consistency of the disk thickness was evaluated. Accordingly, 3 leveling replicates by
226 2 different operators were undertaken. After each of them, a batch of 6 disks was produced. The
227 disks were characterized in terms of weight and thickness, the latter being measured along 3
228 concentric circumferences (Table 1). For each leveling replicate, the mean disk weight ($n = 6$) and
229 the mean disk thickness from the measurements either along each circumference ($n = 6$) or all the 3
230 circumferences ($n = 18$) were calculated, in order to gain information on intra-operation variability.
231 In addition, mean weight and thickness values were calculated considering all samples from
232 different batches ($n = 36$) in order to also take inter-operation variability into account.
233 Good results in terms of continuous flow of the material from the nozzle during the printing process
234 were indicated by the low weight variability ($CV < 2$). However, thickness data poorly complied
235 with the value defined in the CAD file (*i.e.* 600 μm) and showed reproducibility issues. In
236 particular, intra-operation differences (*i.e.* among disks printed following the same leveling) up to
237 about 200 μm and inter-operation differences (*i.e.* among disks printed following 2 different
238 levelings) up to about 400 μm were observed. Because disks are composed of 2 layers only,
239 leveling, which determines the thickness of the former layer by establishing the distance between
240 the nozzle and the build plate, ultimately affects the final thickness. Moreover, these results
241 highlighted inherent resolution limits of the printer, used under standard operating conditions (*e.g.*
242 PLA filament and 0.4 mm tip), which would have to be taken into account when the quality
243 standards of pharmaceutical products need to be fulfilled.

244 With regard to the extrusion of filaments from the selected pharmaceutical grade polymers, the type
245 and amount of plasticizers were adjusted, based on the torque values recorded, to enable continuous
246 extrusion throughout the barrel of the employed equipment that has limited length (12 cm). This
247 would indeed result in relatively short-lasting exposure of the material to the temperature and shear
248 stress conditions that cause its softening/melting. Previous 3DP trials pointed out the need for
249 filaments with a minimum length of 25 cm, circular cross section and proper diameter as well as
250 diameter tolerances (1.75 ± 0.05 mm) (Melocchi et al., 2015b). For the purpose of producing
251 suitable filaments, the twin-screw extruder used was equipped with a custom-made aluminum die
252 having a conical section at the entry side and a cylindrical section at the exit. The extruded
253 filaments were then pulled manually through a gauge of 1.80 mm to maintain the desired diameter.
254 The size of filaments, checked every 5 cm, turned out slightly lower than the PLA one (mean = 1.71
255 mm, CV 2.30 vs 1.79 mm, CV 1.10). Not only the diameter but also the mechanical properties of
256 the filament were critical to 3DP processability. Problems of rupture or wrapping around gears were
257 initially encountered. In order to overcome these issues, the feeding mechanism of the printer was
258 modified by replacing the standard spring with one of lower stiffness, thus reducing the
259 compression force applied and possibly broadening the range of formulations that could be used.
260 When feeding failure still occurred, small increases or decreases in the amount of plasticizer (1%),
261 depending on whether rupturing or wrapping problems had to be faced, respectively, were
262 systematically attempted. This trial and error approach was continued until formulations suitable for
263 both extrusion of filaments and feeding of the printer were attained.

264 The formulation and the extrusion as well as FDM processing conditions relevant to each polymer
265 investigated, along with photographs of the extruded filaments and printed disks, are reported in
266 Table 2.

267 The temperature needed for printing generally turned out to be higher than for extrusion of
268 filaments. This may be due to the short residence time of the material in the heating chamber of the
269 3D printer and, also, to the limited contribution of the shear stress developed by the loading gear, if

270 compared with the counter-rotating twin-screws of the extruder. Problems of nozzle clogging
271 following increase in the melt viscosity, caused by decrease in the FDM processing temperature,
272 were already described (Pietrzak et al., 2015). Moreover, because an unheated build plate was used,
273 as involved by the standard configuration of Makerbot Replicator 2, the temperature of the material
274 flowing out from the heating chamber also needed to compensate for the sudden cooling occurring
275 on deposition, which could hinder proper adherence of the layers to each other and to the surface of
276 the plate. Removal of disks from the build plate without damaging was in all cases possible because
277 of sufficient cohesion between the overlapping layers. The extent of plasticization was found
278 critical in this respect.

279 The printing process took approximately 2 min per disk. Entire printed disks were obtained,
280 wherein the 90° deposition pattern was evident (Table 2). When trying to improve the printing
281 resolution, disks with the required physico-technological characteristics were not always obtained.
282 High-resolution setting necessarily involves decreased rate of deposition and reduced layer
283 thickness, and this may have worsened issues related to sudden cooling of the melt.

284 Weight and thickness data of disks are reported in Table 3.

285 The variability of both weight and thickness turned out increased with respect to disks printed from
286 the Makerbot supplied PLA filament though using the same CAD file. Moreover, the average
287 thickness of the disks based on pharmaceutical grade polymers was generally lower than the
288 nominal value, ranging from less than 500 μm to approximately 600 μm . Such results were partly
289 expected due to the inherent characteristics of each material, such as the rheological behavior when
290 melt and the possible tendency to volumetric changes after hot-processing (Zema et al., 2013a), and
291 could also be ascribed to problems of continuous loading of the equipment. These would depend on
292 the variability in diameter of the filaments produced in-house and their mechanical properties.
293 Besides, such filaments were thinner than the supplied PLA one, ranging on average from 1.70 mm
294 to 1.74 mm in diameter, which would impact on the thickness of the printed layers, especially when
295 considering that the 3D printer is set for a filament of 1.77 mm in diameter. It should be noted that,

296 the possibility of modifying the CAD file to account for the volumetric changes of the material
297 following printing was already exploited with HPC (Melocchi et al., 2015b).

298

299 **3.2 Evaluation of the barrier performance of printed disks**

300 Disks were used as a simple model to evaluate the performance of printed barriers when in contact
301 with aqueous fluids, *i.e.* coatings and capsule shells. For this purpose, the disks were positioned to
302 close purposely-developed cells with a donor compartment that was filled with a drug tracer (Zema
303 et al., 2013b). The assembled cells were immersed in an acceptor medium and tests were carried out
304 in a dissolution apparatus 2. By assaying the drug recovered in the medium over time, cumulative
305 curves were obtained.

306 The behavior of disks based on promptly soluble polymers (*i.e.* KIR and PEO) was first explored
307 (Figure 3). With either polymeric barriers the whole amount of drug was found in the acceptor
308 medium after 15 min of testing. A further improvement in terms of dissolution rate could be
309 achieved by reducing the disk thickness. The dissolution of disks was rapidly completed after their
310 rupturing occurring within 5 and 10 min in the case of KIR and PEO, respectively. Also, mass loss
311 tests, carried out under different hydrodynamic conditions, showed that the printed samples based
312 on both materials entirely dissolved in 3 min. According to these results, KIR and PEO could be
313 employed as main components of coatings or capsules for immediate-release fabricated by FDM.
314 These printed capsules could represent an alternative to the gelatin and HPMC ones currently
315 available.

316 Disks based on the swellable/erodible polymers under investigation displayed the expected delay
317 prior to recovery of the drug tracer in the acceptor medium. Indeed, during the test they showed the
318 typical swelling and erosion/dissolution phenomena upon hydration, until break-up of the barrier.
319 After this lag phase, a fast increase in the amount of drug recovered in the medium was observed.

320 Such a pattern is typical of DDSs for pulsatile release. By way of example, individual profiles
321 relevant to HPMC-based disks are shown in Figure 4.

322 The curves presented are characterized by different lag times ($t_{10\%} \approx 65, 75$ and 85 min). Such
323 differences would at least partly be due to the diverse thickness values of each sample, *i.e.* $482 \mu\text{m}$
324 (CV 7.6); $582 \mu\text{m}$ (CV 6.1), $603 \mu\text{m}$ (CV 3.2). The influence of the barrier thickness and of the
325 physico-chemical properties of the selected polymers on lag time is well-known and has largely
326 been demonstrated in the case of swellable/erodible reservoir systems prepared by IM, film-coating,
327 powder-layering and compression coating (Del Curto et al., 2014; Gazzaniga et al., 2011; Maroni et
328 al., 2013a and b; Maroni et al., 2016; Sangalli et al., 2009; Zema et al., 2013a). In order to compare
329 printed disks based on the various polymers investigated, a previously introduced index was
330 employed, the time equivalent thickness parameter (TETP), which expresses the thickness of a
331 polymeric layer needed to attain a lag time of 1 min (Table 4) (Sangalli et al., 2004). As expected,
332 TETP values pointed out a different efficiency of these polymers. The behavior of printed disks
333 based on SLP, purposely developed for the achievement of solid dispersions of poorly-soluble
334 drugs by HME, was comparable with that of barriers based on swellable polymers of established
335 use in the manufacturing of DDSs for pulsatile release.

336 The overall results pointed out the availability of a number of hydrophilic polymers other than HPC
337 that could be suitable for printing capsule shells and for modulating the onset of drug release
338 (Melocchi et al., 2015b).

339 From EC and EDR RL, poorly-permeable insoluble disks were obtained. Indeed, the amount of
340 drug recovered in the acceptor fluid increased very slowly, particularly when dealing with the EC
341 barrier (Figure 5). In this respect, although hot-processing techniques are known to lead to high-
342 density structures, FDM may grant the possibility of achieving different porosity characteristics
343 based on printing parameters, such as primarily on how close the layers are deposited (Loreti et al.,
344 2014; Melocchi et al., 2015a). The addition of channeling agents into the filament formulation may
345 also enhance the barrier permeability. The low rate of drug permeation could also be attributed to

346 the relatively high thickness of the printed disks as compared with films commonly applied to solid
347 dosage forms in order to prolong the drug release over time. Fabrication of thinner barriers, which
348 would most likely be intended for using as coatings rather than capsule shells, could represent a
349 further strategy to achieve release rates consistent with the oral administration route.

350 Finally, the barriers based on enteric soluble polymers, *i.e.* HPMCAS and EDR L, were evaluated
351 by using HCl 0.1 N and then phosphate buffer pH 6.8 as the acceptor fluids. The disks showed the
352 expected resistance when in contact with the acidic medium. When switching to phosphate buffer, a
353 lag time elapsed before dissolution and consequent rupture of the barriers. Such lag time was of
354 40.42 min (CV 7.32) and 45.95 min (CV 12.23) with HPMCAS and EDR L, respectively. From
355 HPMCAS-based disks and capsular devices manufactured by IM, a lag time before dissolution of
356 the enteric soluble polymer was analogously observed (Zema et al., 2013b). In that case, the time
357 taken for this process was shortened by adding channeling agents and/or reducing the thickness of
358 molded barriers, which could also be exploited with 3D printed items.

359

360 **3.3 Printing and evaluation of double-disk items**

361 In order to preliminarily evaluate the feasibility of FDM in the fabrication of coated dosage forms, a
362 double-disk item was obtained by successively printing two overlaid disks of different composition,
363 with no need for a newly designed CAD file. The filament for the former disk was extruded starting
364 from the KIR-based formulation containing furosemide (30% by weight), a poorly-soluble active
365 ingredient having high-melting point. The hot-processability of this model drug was already
366 demonstrated when mixed with the same polymer (Melocchi et al., 2015a). The latter disk was
367 based on HPMCAS.

368 The impact of the drug on the process parameters and quality of the product was negligible not only
369 as regards HME, as expected on the basis of previous experience, but also in the case of FDM.

370 After printing of the former disk, the remainder of the material was completely removed from the

371 heating chamber of the 3D printer by a purge operation before feeding the latter filament, which
372 required to be processed at a higher temperature. Re-leveling was then performed with respect to
373 the printed furosemide-containing disk. At the end of the process, the two parts of the double-disk
374 item tightly adhered to each other, and the overall thickness was of 1052 μm (CV 12.7). For
375 comparison purposes, single-disks containing furosemide were also printed.

376 Double-disk items were positioned into the cells for evaluation of performance, so that the enteric-
377 soluble side was in contact with the medium and the drug-containing one was oriented towards the
378 empty donor compartment. During the acidic stage of the test no drug was recovered in the acceptor
379 medium, thus indicating that gastroresistance was effective (Figure 6). In the pH 6.8 fluid, the drug
380 was released after a lag phase ($t_{10\%} = 49.06$ min, CV 6.26) that turned out comparable in duration
381 with that previously assessed when testing the HPMCAS disks as such. Moreover, the release
382 pattern after the lag phase was analogous to that obtained from single furosemide-containing disks.
383 These are the typically results that are observed from enteric-coated dosage forms.

384

385 **4. Conclusions**

386 Filaments based on a variety of pharmaceutical grade polymers, *i.e.* Kollicoat[®] IR, PEO, HPC,
387 HPMC, PVA, Soluplus[®], EC, Eudragit[®] RL, Eudragit[®] L and HPMCAS, were successfully
388 produced, which turned out suitable for 3D printing by FDM. From filaments based on all these
389 materials, disk-shaped specimens having thickness on the order of hundreds of microns were
390 obtained. The printed disks were proved advantageous to investigate both the processability of the
391 polymers and their behavior in contact with aqueous fluids after processing. When used as barriers,
392 such disks performed as promptly-soluble, swellable/erodible, slowly-permeable insoluble and
393 gastroresistant layers, consistent with the nature of their polymeric components and main
394 applications in pharmaceutical formulation. Moreover, multiple overlaid disks were shown feasible.
395 Overall, the potential of the investigated materials when processed by FDM was demonstrated for
396 the manufacturing of immediate-release capsules, delivery platforms based on capsular devices and

397 cosmetic or functional coating layers. In addition, a variety of further products, such as tablets and
398 matrices, could be obtained by incorporating active ingredients into the filaments.

399 As occurred in the past when transferring other industrial technologies to the pharmaceutical field
400 (*e.g.* pelletization, HME, IM), a full exploitation of FDM and relevant broad application in this area
401 actually require the development of suitable equipment and processes, which would enable the
402 manufacturing of products complying with the strict quality standards involved.

403

404 **5. References**

405 Del Curto M. D., Palugan L., Foppoli A., Zema L., Gazzaniga A., Maroni A., Erodible time-
406 dependent colon delivery systems with improved efficiency in delaying the onset of drug release, *J.*
407 *Pharm. Sci.*, 103: 3585-3593 (2014).

408 Gazzaniga A., Cerea M., Cozzi A., Foppoli A., Maroni A., Zema L., A novel injection-molded
409 capsular device for oral pulsatile delivery based on swellable/erodible polymers, *AAPS*
410 *PharmSciTech.*, 12: 295-303 (2011).

411 Genina N., Holländer J., Jukarainen H., Mäkilä E., Salonen J., Sandler N., Ethylene vinyl acetate
412 (EVA) as a new drug carrier for 3D printed medical drug delivery devices, *Eur. J. Pharm. Sci.*,
413 <http://dx.doi.org/10.1016/j.ejps.2015.11.005> (2016).

414 Gibson I., Rosen D. W., Stucker B., *Additive Manufacturing Technologies: rapid prototyping to*
415 *direct digital manufacturing*, Springer, New York (2010).

416 Giordano F., Rossi A., Bettini R., Savioli A., Gazzaniga A., Novák Cs., Thermal behavior of
417 paracetamol polymeric excipients mixtures, *J. Therm. Anal. Calorim.*, 68: 575-590 (2002).

418 Goyanes A., Buanz A. B. M., Basit A. W., Gaisford S., Fused-filament 3D printing (3DP) for
419 fabrication of tablets, *Int. J. Pharm.*, 476: 88-92 (2014).

420 Goyanes A., Robles Martinez P., Buanz A., Basit A. W., Gaisford S., Effect of geometry on drug
421 release from 3D printed tablets , *Int. J. Pharm.*, 494: 657-663 (2015a).

422 Goyanes A., Chang H., Sedough D., Hatton G. B., Wang J., Buanz A., Gaisford S., Basit A. W.,
423 Fabrication of controlled-release budesonide tablets via desktop (FDM) 3D printing, *Int. J. Pharm.*,
424 496: 414-420 (2015b).

425 Goyanes A., Wang J., Buanz A., Martínez-Pacheco R., Telford R., Gaisford S., Basit A. W., 3D
426 Printing of medicines: engineering novel oral devices with unique design and drug release
427 characteristics, *Mol. Pharm.*, 12: 4077-4084 (2015c).

428 Goyanes A., Buanz A. B. M., Hatton G. B., Gaisford S., Basit A. W., 3D printing of modified-
429 release aminosalicylate (4-ASA and 5-ASA) tablets, *Eur. J. Pharm. Biopharm.*, 89: 157-162
430 (2015d).

431 Holländer J., Genina N., Jukarainen H., Khajeheian M., Rosling A., Mäkilä E., Sandler N., Three-
432 dimensional printed PCL-based implantable prototypes of medical devices for controlled drug
433 delivery, *J. Pharm. Sci.*, doi:10.1016/j.xphs.2015.12.012 (2016).

434 [http://www.drugs.com/newdrugs/fda-approves-spritam-levetiracetam-first-3d-printed-product-](http://www.drugs.com/newdrugs/fda-approves-spritam-levetiracetam-first-3d-printed-product-4240.html)
435 [4240.html](http://www.drugs.com/newdrugs/fda-approves-spritam-levetiracetam-first-3d-printed-product-4240.html) (accessed on 04/05/2016).

436 <http://www.spritam.com> (accessed on 04/05/2016).

437 Loreti G., Maroni A., Del Curto M. D., Melocchi A., Gazzaniga A., Zema L., Evaluation of hot
438 melt extrusion technique in the production of HPC matrices for prolonged release, *Eur. J. Pharm.*
439 *Sci.*, 52: 77-85 (2014).

440 Macchi E., Zema L., Maroni A., Gazzaniga A., Felton L. A., Enteric-coating of pulsatile-release
441 HPC capsules prepared by injection molding, *Eur. J. Pharm. Sci.*, 70: 1-11 (2015).

442 Maroni A., Zema L., Del Curto M. D., Foppoli A., Gazzaniga A., Oral colon delivery of insulin
443 with the aid of functional adjuvants, *Adv. Drug Deliv. Rev.*, 64: 540-556 (2012).

444 Maroni A., Zema L., Loreti G., Palugan L., Gazzaniga A., Film coatings for oral pulsatile release,
445 *Int. J. Pharm.*, 457: 362-371 (2013a).

446 Maroni A., Del Curto M. D., Zema L., Foppoli A., Gazzaniga A., Film coatings for oral colon
447 delivery, *Int. J. Pharm.*, 457: 372-394 (2013b).

448 Maroni A., Zema L., Cerea M., Foppoli A., Palugan L., Gazzaniga A., Erodible drug delivery
449 systems for time-controlled release into the gastrointestinal tract, *J. Drug Deliv. Sci. Technol.*, 32:
450 229-235 (2016).

451 Mascia S., Heider P. L., Zhang H., Lakerveld R., Benyahia B., Barton P. I., Braatz R. D., Cooney
452 C. L., Evans J. M. B., Jamison T. F., Jensen K. F., Myerson A. S., Trout B. L., End-to-end
453 continuous manufacturing of pharmaceuticals: integrated synthesis, purification, and final dosage
454 formation, *Angew. Chem. Int. Ed. Engl.*, 52: 12359-12363 (2013).

455 Melocchi A., Loreti G., Del Curto M. D., Maroni A., Gazzaniga A., Zema L., Evaluation of hot
456 melt extrusion and injection molding for continuous manufacturing of immediate release tablets, *J.*
457 *Pharm. Sci.*, 104: 1971-1980 (2015a).

458 Melocchi A., Parietti F., Loreti G., Maroni A., Gazzaniga A., Zema L., 3D printing by fused
459 deposition modeling (FDM) of a swellable/erodible capsular device for oral pulsatile release of
460 drugs, *J. Drug. Deliv. Sci. Technol.*, 30 Part B: 360-367 (2015b).

461 Norman J., Madurawe R. D., Moore C. M. V., Khan M. A., Khairuzzaman A., A new chapter in
462 pharmaceutical manufacturing: 3D-printed drug, *Adv. Drug Deliv. Rev.*,
463 doi:10.1016/j.addr.2016.03.001 (2016).

464 Park K., 3D printing of 5-drug polypill, *J. Control. Release*, 217: 352 (2015).

465 Pietrzak K., Isreb A., Alhnan M. A., A flexible-dose dispenser for immediate and extended release
466 3D printed tablets, *Eur. J. Pharm. Biopharm.*, 96: 380-387 (2015).

467 Pham D. T., Gault R. S., A comparison of rapid prototyping technologies, *Int. J. Mach. Tools*
468 *Manuf.*, 38: 1257-1287 (1998).

469 Prasad L. K., Smyth H., 3D Printing technologies for drug delivery: a review, *Drug Dev. Ind.*
470 *Pharm.*, 13: 1-13 (2015).

471 Rengier F., Mehndiratta A., von Tengg-Kobligk H., Zechmann C. M., Unterhinninghofen R.,
472 Kauczor H. U., Giesel F. L., 3D printing based on imaging data: review of medical applications, *Int.*
473 *J. Comput. Assist. Radiol. Surg.*, 5: 335-341 (2010).

474 Sandler N., Salmela I., Fallarero A., Rosling A., Khajeheian M., Kolakovic R., Genina N., Nyman
475 J., Vuorela P., Towards fabrication of 3D printed medical devices to prevent biofilm formation, *Int.*
476 *J. Pharm.*, 459: 62-64 (2014).

477 Sangalli M. E., Maroni A., Foppoli A., Zema L., Giordano F., Gazzaniga A., Different HPMC
478 viscosity grades as coating agents for an oral time and/or site-controlled delivery system: a study on
479 process parameters and in vitro performances, *Eur. J. Pharm. Sci.*, 22: 469-476 (2004).

480 Sangalli M. E., Maroni A., Zema L., Cerea M., Gazzaniga A., The Chronotopic™ technology, in:
481 B.-B.C. Youan (Ed.), *Chronopharmaceutics. Science and technology for biological rhythm guided*
482 *therapy and prevention of diseases*, John Wiley&Sons, Hoboken, New Jersey, pp. 145-163 (2009).

483 Skowrya J., Pietrzak K., Alhnan M. A., Fabrication of extended-release patient-tailored
484 prednisolone tablets via fused deposition modelling (FDM) 3D printing, *Eur. J. Pharm. Sci.*, 68: 11-
485 17 (2015).

486 Shah S., Maddineni S., Lu J., Repka M. A., Melt extrusion with poorly soluble drugs, *Int. J. Pharm.*,
487 453: 233-52 (2013).

488 Water J. J., Bohr A., Boetker J., Aho J., Sandler N., Nielsen H. M., Rantanen J., Three-dimensional
489 printing of drug-eluting implants: preparation of an antimicrobial polylactide feedstock material, *J.*
490 *Pharm. Sci.*, 104:1099-1107 (2015).

491 Yu D. G., Zhu L. M., Branford-White C. J., Yang X. L., Three-dimensional printing in
492 pharmaceuticals: promises and problems, *J. Pharm. Sci.*, 97: 3666-3690 (2008).

493 Zema L., Loreti G., Melocchi A., Maroni A., Gazzaniga A., Injection molding and its application to
494 drug delivery, *J. Control. Release*, 159: 324-331 (2012).

495 Zema L., Loreti G., Melocchi A., Maroni A., Palugan L., Gazzaniga A., Gastroresistant capsular
496 device prepared by injection molding, *Int. J. Pharm.*, 440: 264-272 (2013b).

497 Zema L., Loreti G., Macchi E., Foppoli A., Maroni A., Gazzaniga A., Injection-molded capsular
498 device for oral pulsatile release: development of a novel mold, *J. Pharm. Sci.*, 102: 489-499
499 (2013a).

Table 1: weight and thickness of PLA disks fabricated after 3 leveling of the build plate by 2 different operators

	Leveling replicate	Weight mg (CV) <i>n</i> = 6	Thickness μm (CV)			
			Outer circumference <i>n</i> = 6	Intermediate circumference <i>n</i> = 6	Inner circumference <i>n</i> = 6	All circumferences <i>n</i> = 18
Operator 1	I	514.6 (1.7)	636 (4.1)	626 (5.1)	622 (5.2)	628 (4.8)
	II	514.4 (0.5)	680 (5.6)	665 (4.6)	673 (6.6)	673 (5.6)
	III	520.9 (0.2)	720 (8.0)	706 (5.6)	724 (8.9)	717 (7.6)
Operator 2	I	507.5 (1.3)	643 (6.9)	633 (4.7)	635 (5.6)	637 (5.7)
	II	525.4 (0.2)	737 (5.0)	736 (6.3)	739 (3.6)	738 (4.9)
	III	533.9 (0.2)	844 (8.9)	838 (7.2)	832 (7.2)	832 (7.8)
All leveling replicates <i>n</i> = 36		519.5 (1.8)	710 (12.0)	701 (11.8)	701 (11.0)	704 (11.7)

Table 2: formulation, process parameters and photographs relevant to extruded filaments and printed disks (entire and magnified detail) based on different pharmaceutical grade polymers





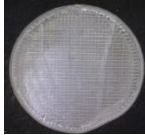


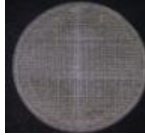





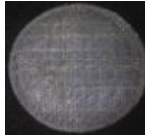

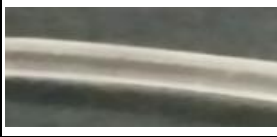




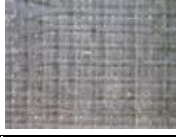


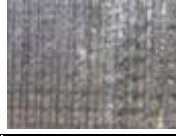




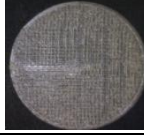

FORMULATION	HME				FDM		
	T (°C)	Screw speed (rpm)	Torque (N·cm)	Product 5 mm	T (°C)	Product 10 mm	x 10 magnification
KIR + 12% GLY	160	100	80		180		
PEO	65	100	100		160		
HPMC + 5% PEG 400	160	70	70		200		
HPC	165	80	40		180		
PVA+ 5% GLY	190	70	80		225		
SLP + 10% PEG 400	120	80	80		200		
HPMCAS + 5% PEG 8000	180	100	100		200		
EDR L + 20% TEC	160	80	120		160		
EDR RL + 15% TEC	120	95	60		160		
EC + 10% TEC	160	100	100		200		

Table 3: weight and thickness data of printed disks based on different pharmaceutical grade polymers

FORMULATION	Weight mg (CV)	Thickness µm (CV)			
		Outer circumference <i>n</i> = 6	Intermediate circumference <i>n</i> = 6	Inner circumference <i>n</i> = 6	All circumferences <i>n</i> = 18
KIR + 12% GLY	477.4 (3.8)	634 (9.2)	601 (5.7)	623 (7.6)	614 (7.5)
PEO	364.0 (12.8)	571 (10.6)	563 (11.2)	555 (14.0)	563 (11.9)
HPMC + 5% PEG 400	435.7 (9.2)	605 (12.8)	559 (10.7)	526 (12.7)	563 (11.4)
HPC	423.3 (2.0)	645 (5.9)	635 (6.2)	634 (5.2)	638 (5.8)
PVA+ 5% GLY	352.0 (10.3)	528 (8.9)	545 (12.8)	527 (6.5)	533 (9.9)
SLP + 10% PEG 400	325.0 (13.6)	543 (18.0)	540 (17.1)	528 (21.6)	537 (18.8)
HPMCAS + 5% PEG 8000	373.5 (5.8)	504 (11.8)	479 (15.0)	450 (12.9)	478 (13.9)
EDR L + 20% TEC	354.0 (9.0)	486 (14.6)	474 (13.5)	468 (11.6)	476 (13.4)
EDR RL + 15% TEC	336.9(5.9)	660 (13.1)	660 (11.9)	683 (10.1)	668 (11.8)
EC + 10% TEC	442.7 (4.8)	629 (6.1)	620 (5.9)	623 (5.8)	624 (5.9)

Table 4: TETP from disks based on swellable/erodible polymers

FORMULATION	TETP μm/min (CV)
HPMC + 5% PEG 400	7.36 (0.33)
SLP + 10% PEG 400	15.54 (2.28)
HPC	22.42 (4.17)
PVA + 5% GLY	37.84 (2.05)

Figure 1: image of a printed disk reporting the 3 concentric circumferences along which thickness was measured (outer circumference, white; intermediate circumference, grey; inner circumference, black)

Figure 2: test cells before assembly (a) and after filling of the reservoir donor compartment with AAP powder (b), positioning of the disk (c) and final assembly (d)

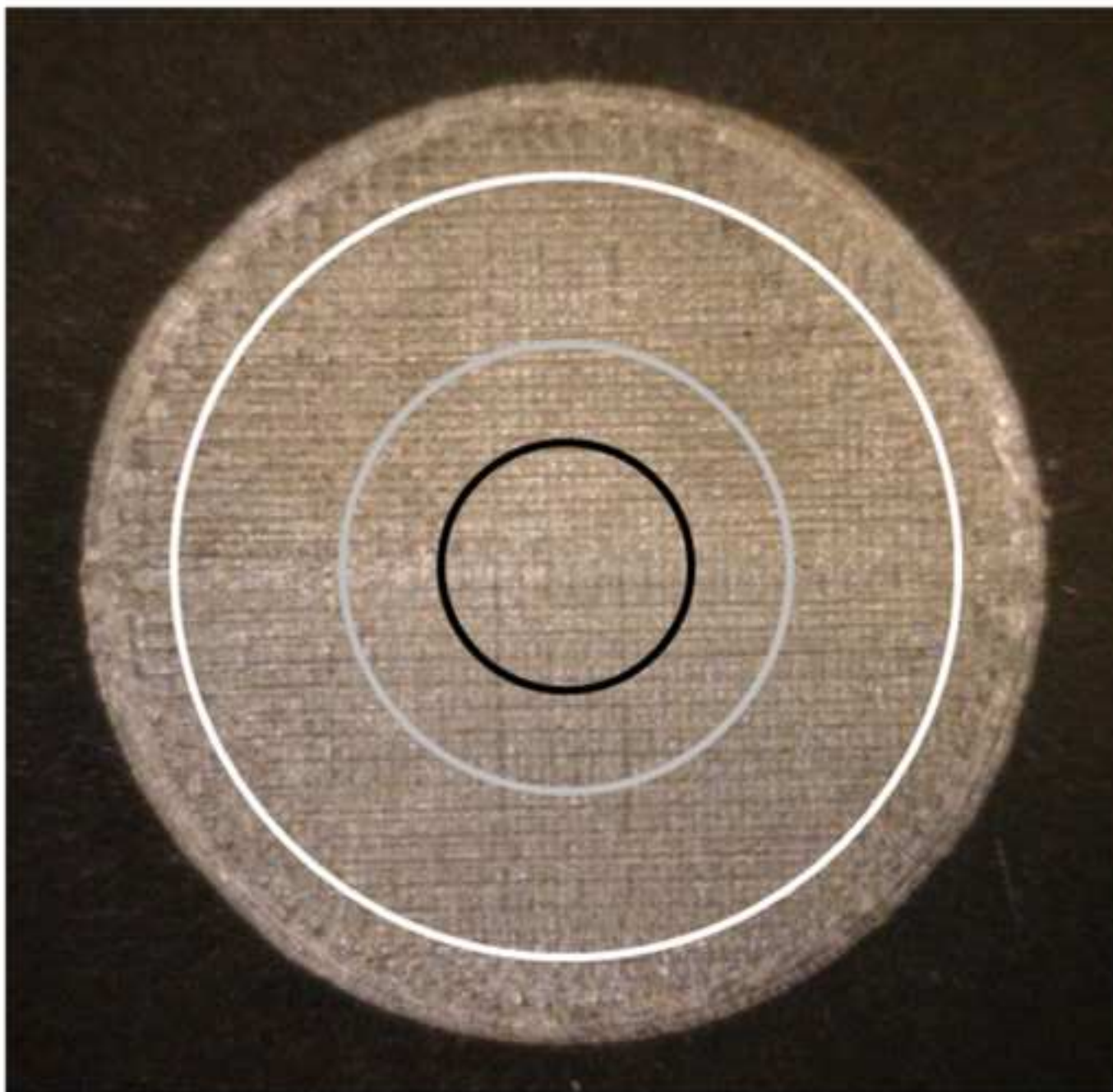
Figure 3: drug recovered *vs* time profiles obtained from disks based on promptly soluble polymers

Figure 4: individual drug recovered *vs* time profiles obtained from disks based on HPMC

Figure 5: drug recovered *vs* time profiles obtained from disks based on insoluble polymers

Figure 6: drug recovered *vs* time profiles obtained from single (a) and double (b) disks containing furosemide; lateral views of disks are also reported

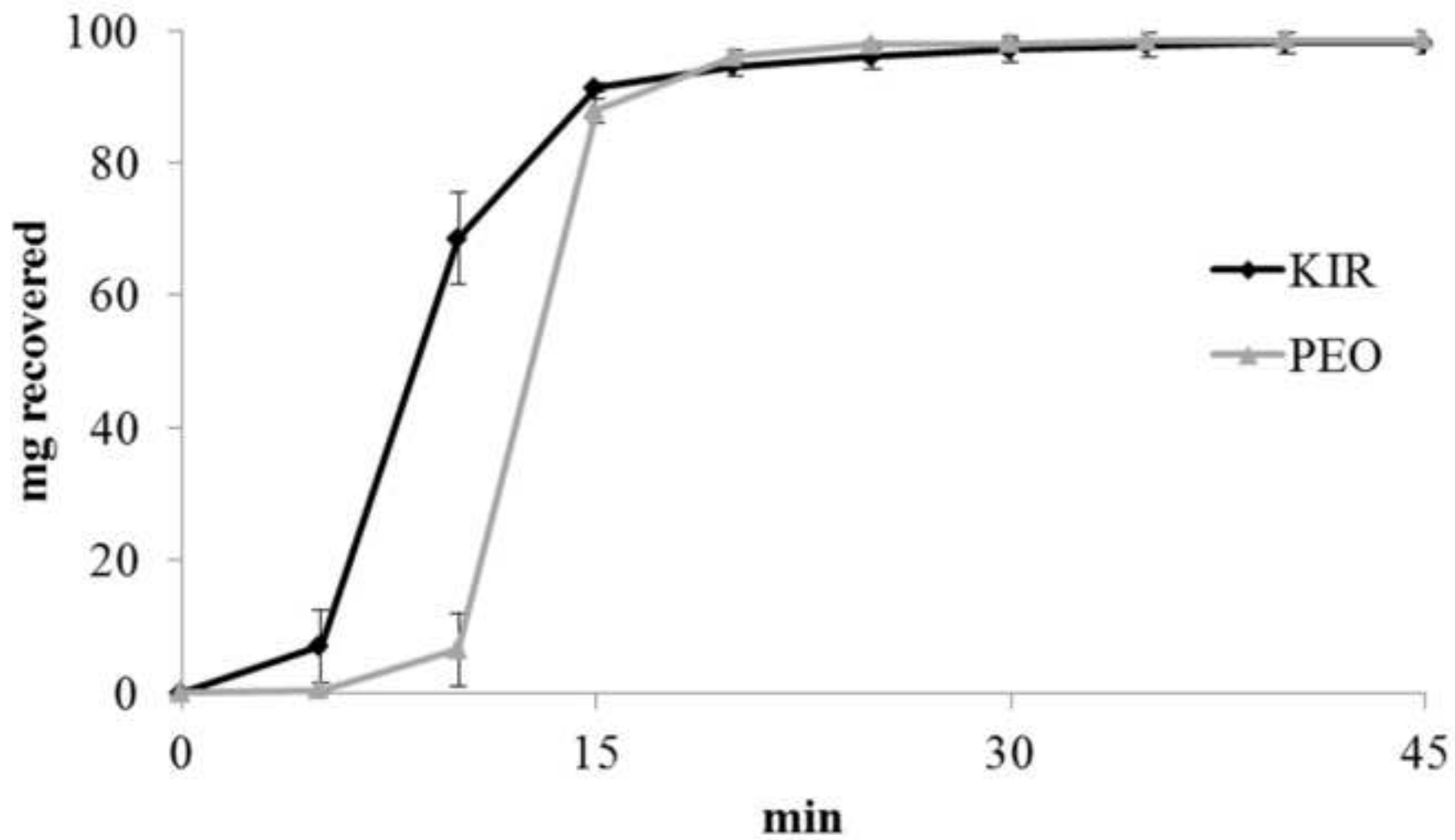
Figure(s)



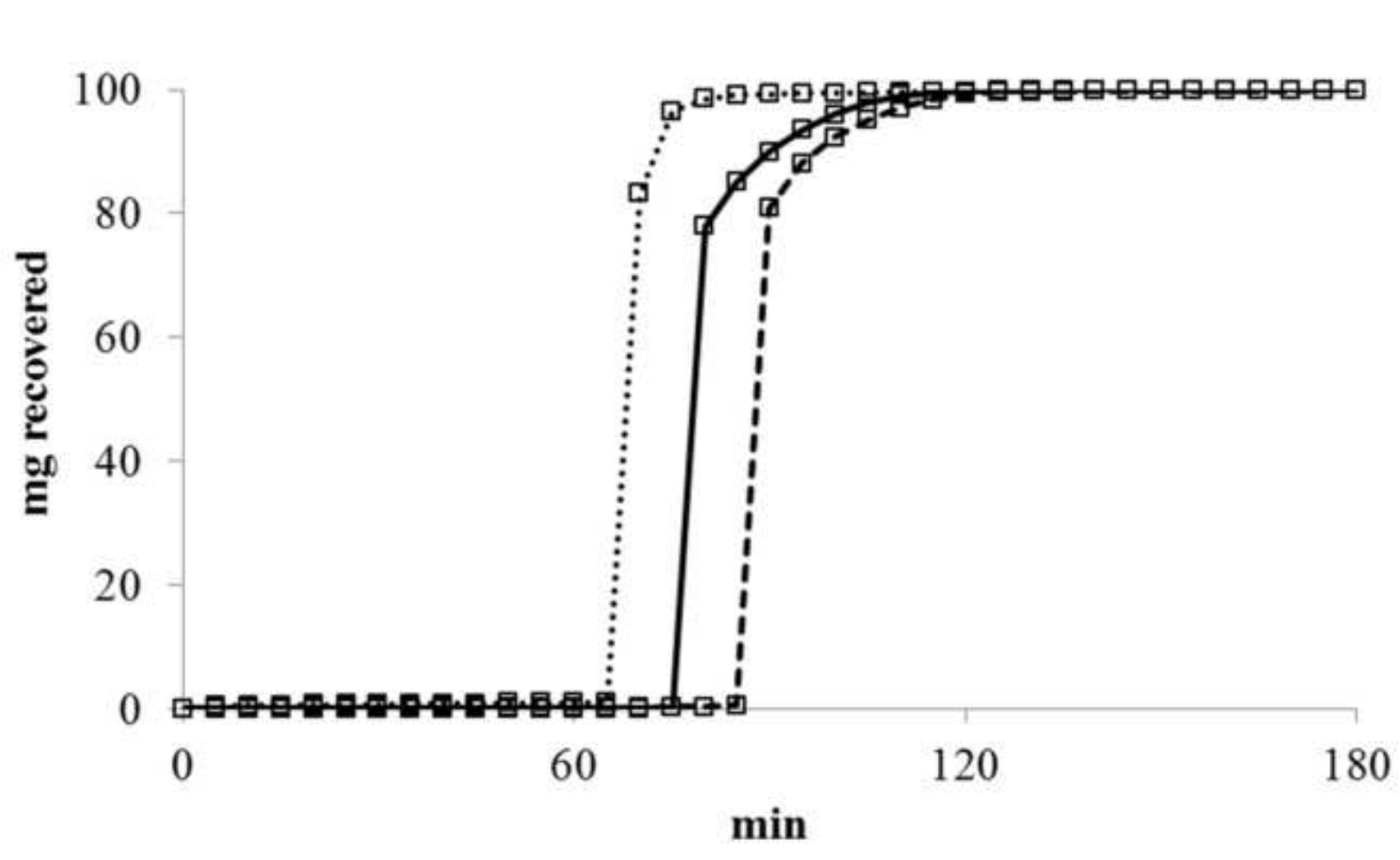
Figure(s)



Figure(s)



Figure(s)



Figure(s)

